

# Air-Processable Silane-Coupled Polymers to Modify a Dielectric for Solution-Processed Organic Semiconductors

Mi Jang,<sup>†</sup> Young Chang Yu,<sup>†</sup> Hyeonyeol Jeon,<sup>‡</sup> Ji Ho Youk,<sup>\*,†</sup> and Hoichang Yang<sup>\*,†</sup>

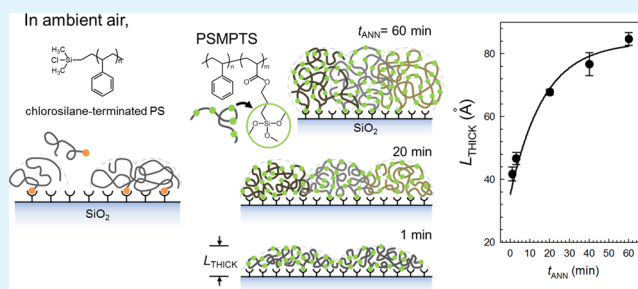
<sup>†</sup>Department of Applied Organic Materials Engineering, Inha University, Incheon 402-751, Republic of Korea

<sup>‡</sup>Center for Materials Architecturing, Korea Institute of Science and Technology, Seoul 136-794, Republic of Korea

## Supporting Information

**ABSTRACT:** Poly(styrene-*r*-3-methacryloxypropyltrimethoxysilane) (PSMPTS) copolymers were synthesized by the free radical polymerization of styrene and 3-methacryloxypropyltrimethoxysilane (MPTS) for use as surface modifiers. PSMPTS copolymers were spun-cast onto a hydrophilic SiO<sub>2</sub> layer and were then annealed at 150 °C in ambient air. The polystyrene (PS)-based copolymer, with a molecular weight of 32 700 g mol<sup>-1</sup> and approximately 30 MPTS coupling sites, was easily grafted onto the SiO<sub>2</sub> surface after annealing periods longer than 1 min, yielding a physicochemically stable layer. On the untreated and polymer-treated dielectrics, spin-casting of an ultrasonicated poly(3-hexyl thiophene) (P3HT) solution yielded highly interconnected crystal nanofibrils of P3HT. The resulting organic field-effect transistors (OFETs) showed similar mobility values of 0.01–0.012 cm<sup>2</sup> V<sup>-1</sup> s<sup>-1</sup> for all surfaces. However, the threshold voltage ( $V_{th}$ ) drastically decreased from +13 (for bare SiO<sub>2</sub>) to 0 V by grafting the PSMPTS copolymers to the SiO<sub>2</sub> surface. In particular, the interfacial charge traps that affect  $V_{th}$  were minimized by grafting the 11 mol % MPTS-loaded copolymer to the polar dielectric surface. We believe that this ambient-air-processable silane-coupled copolymer can be used as a solution-based surface modifier for continuous, large-scale OFET fabrication.

**KEYWORDS:** silane polymer, polymer grafting, solution-processable semiconductor, poly(3-hexyl thiophene), organic field-effect transistor



## 1. INTRODUCTION

Organic field-effect transistors (OFETs) have received considerable attention over the past decade owing to their potential applications in integrated circuits, including radio frequency identification tags, smart cards, sensors, and organic active matrix displays.<sup>1–7</sup> The field-effect mobility ( $\mu_{FET}$ ) of OFETs is clearly comparable to that of amorphous silicon-based devices.<sup>8–12</sup> During the last two decades,  $\mu_{FET}$  values of polymer field-effect transistors (FETs) have increased significantly from less than 10<sup>-3</sup> cm<sup>2</sup> V<sup>-1</sup> s<sup>-1</sup> to more than 10 cm<sup>2</sup> V<sup>-1</sup> s<sup>-1</sup>, which exceeds those of amorphous silicon FETs.<sup>10,13</sup> These improvements are mainly related to the drastic enhancement in both intra- and intermolecular conjugation lengths of organic semiconductors via novel synthetic approaches or optimization of the interface engineering between organic semiconductors and dielectrics.<sup>10,13</sup> It is well-known that the charge-carrier transport in OFETs is vertically confined to ultrathin semiconducting layers (<5 nm) near the gate dielectrics.<sup>8,14</sup> Also, the surface properties of dielectrics are major factors that determine the number of interfacial trap sites originating from polar surface moieties, less-conjugated crystallites of semiconducting polymers, and grain boundaries (GB).<sup>11,12,15</sup> Therefore, organo-compatible dielectrics with fewer trap sites are necessary to achieve high-performance solution-processed OFETs.

Nonpolar self-assembled monolayers (SAMs) or common polymer thin films can induce organo-compatible dielectric surfaces with fewer charge-trapping sites.<sup>11,12,16,17</sup> End-functionalized polymers have been extensively used as surface-grafting modifiers in surface- and interface-related nanoscience and nanotechnology.<sup>11,12,18–20</sup> Yang and co-workers have reported that the organo-compatibility of hydroxyl-rich oxide or polymer dielectrics could be improved through grafting of chlorosilane-end coupled polystyrene (PS) to these surfaces.<sup>11,12,18</sup> In this case, the grafted polymer-layers maintained excellent solvent resistance without any dewetting or delaminating, even under direct solvent contact. Generally, end-functionalized polymers in dried films tend to be slowly grafted even at high temperatures because there is only one coupling site present on each polymeric molecule. In particular, ambient-air conditions, such as oxygen and humidity levels, should be carefully controlled to avoid the deactivation of limited coupling sites, particularly for air-sensitive chlorosilane-terminated polymers.<sup>21</sup>

Unlike these one-point coupling polymers, binary vinyl copolymers containing multiple coupling sites can be quickly

**Received:** December 5, 2014

**Accepted:** February 20, 2015

**Published:** February 20, 2015

grafted to various oxide surfaces.<sup>22–25</sup> One of the most important coupling agents is 3-methacryloxypropyltrimethoxysilane (MPTS). Copolymers containing MPTS have been easily copolymerized with various vinyl monomers and used for the practical adhesion of polymers to minerals.<sup>22–25</sup>

To develop an ambient-air grafting method of silane-coupled polymer chains to hydroxyl-group containing oxide or polymer surfaces, we synthesized poly(styrene-*r*-3-methacryloxypropyltrimethoxysilane) (PSMPTS) copolymers containing 5–11 mol % MPTS by free radical polymerization. PSMPTS copolymers were dissolved in toluene and the solutions were spun-cast onto 300 nm-thick SiO<sub>2</sub> dielectrics. The polymer films were then annealed at 150 °C to thermally graft the polymer chains to the SiO<sub>2</sub> surface. Finally, the annealed films were subsequently rinsed with excess toluene. On the untreated and polymer-grafted SiO<sub>2</sub> dielectrics, well-dispersed nanofibrillar networks of poly(3-hexyl thiophene) (P3HT) were formed via spin-casting a previously ultrasonicated P3HT solution. The resulting P3HT-based OFETs showed not only similar  $\mu_{\text{FET}}$  values of 0.01–0.012 cm<sup>2</sup> V<sup>-1</sup> s<sup>-1</sup> but also significant changes in threshold voltage ( $V_{\text{th}}$ ) ranging from +13 V (untreated) to 0 V (polymer-treated). In particular, the 11 mol % MPTS-loaded copolymer with approximately 30 coupling sites was uniformly grafted to the SiO<sub>2</sub> dielectric surface, even under ambient air. The grafted polymer layer allowed reliable fabrication of a P3HT OFET with  $V_{\text{th}}$  equaling approximately 0 V and negligible hysteresis. We believe that the ambient-air processable silane-coupled PSMPTS copolymers can be used as a dielectric modifier for SiO<sub>2</sub> dielectrics for continuous, solution-processed OFET applications.

## 2. EXPERIMENTAL SECTION

**2.1. Materials and Device Preparation.** Styrene (St, Aldrich, ≥ 99%) was passed through neutral alumina, dried over calcium hydride, distilled under reduced pressure, and degassed using three freeze–pump–thaw cycles. This purification process was also performed for anisole (Junsei, 98.0%), MPTS (TCI, 98.0%), and 2,2'-azobis(4-methoxy-2,4-dimethylvaleronitrile) (V-70, Wakko, 96%). P3HT was synthesized via the Grignard metathesis method with a Ni(dppp)Cl<sub>2</sub> catalyst;<sup>26</sup> the other reagents were used without purification. PSMPTS copolymers with different compositions were synthesized by using various monomer feed ratios ([St]<sub>0</sub>/[MPTS]<sub>0</sub>) = 99/1–97/3, see Figure 1). As a typical example, St (1 mL, 8.7 mmol), MPTS

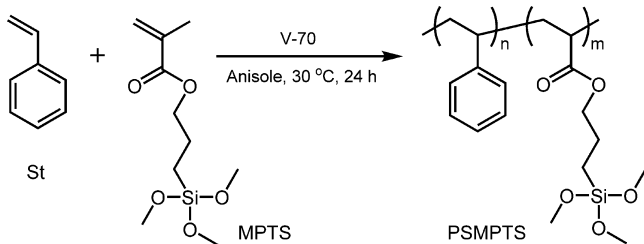


**Figure 1.** Synthesis of poly(styrene-*r*-3-methacryloxypropyltrimethoxysilane) (PSMPTS) copolymer.

(0.0219 g, 0.088 mmol), and V-70 (0.0093 g, 1 wt % of total monomer) were dissolved in 1 mL of anisole under a nitrogen atmosphere. The mixture was purged with nitrogen for 10 min and polymerized at 30 °C for 24 h. The resulting product was diluted with tetrahydrofuran (Duksan, >99.5%) and precipitated in a large amount of methanol. The precipitated polymer was collected by filtration and was dried under vacuum for 24 h.

A 300 nm-thick SiO<sub>2</sub> layer thermally grown onto a highly *n*-doped Si substrate was used as a gate dielectric. The SiO<sub>2</sub>/Si substrates were

first cleaned in boiling acetone, and then UV-ozone (UVO<sub>3</sub>)-treated for 30 min. In ambient air, the solutions of PSMPTS copolymers in toluene were spun-cast onto the hydroxyl-groups presenting SiO<sub>2</sub> surfaces. Dimethylchlorosilane-terminated PS (PS-Si(CH<sub>3</sub>)<sub>2</sub>Cl, number-average molecular weight,  $M_n$  = 26 000 g mol<sup>-1</sup>, i.e., 26 kDa), was also used as a reference polymer. The 20–30 nm thick films were annealed at 150 °C for different annealing times ( $t_{\text{ANN}}$ ) ranging from 0 to 60 min. Then, the annealed films were solvent-rinsed with an excess of toluene to remove any unreacted polymer residue.

A 0.2 wt % solution of P3HT in toluene was ultrasonicated at 18 °C for 10 min to develop highly crystalline nanofibrils, and then P3HT films were spun-cast on untreated and polymer-treated SiO<sub>2</sub> substrates from the ultrasonicated solution. Finally, top contact electrodes were fabricated by thermally evaporating Au through a shadow mask (channel length,  $L$  = 100  $\mu\text{m}$ ; channel width,  $W$  = 1500  $\mu\text{m}$ ) onto the P3HT layers.

**2.2. Characterization.** The molecular weights and distribution of the polymers produced were determined with gel permeation chromatography (GPC, JASCO PU-2080 plus SEC) calibrated with a PS standard series. The level of monomer conversion was determined using a gravimetric method and the polymer composition was determined using <sup>1</sup>H nuclear magnetic resonance (NMR, Bruker Ascend 400, 400 MHz) analysis. Thermal behavior of the PSMPTS series was measured using differential scanning calorimetry (DSC, Q20, TA Instruments). The morphology, thickness, and surface hydrophobicity of the PSMPTS-treated SiO<sub>2</sub> dielectrics were characterized using atomic force microscopy (AFM, Multimode 8, Bruker), X-ray reflectivity (XRR, beamline X9, Brookhaven National Laboratory, USA), and water contact angle measurements, respectively. The crystalline structures of P3HT on the gate dielectrics were investigated using AFM and synchrotron-based grazing-incidence X-ray diffraction (GIXD, beamline 9A, Pohang Acceleration Laboratory, Korea). Electrical characteristics of all the P3HT OFETs were measured in a N<sub>2</sub>-purged glovebox (H<sub>2</sub>O < 0.1 ppm; O<sub>2</sub> < 0.1 ppm) at room temperature using a Keithley 4200 SCS. Values of  $\mu_{\text{FET}}$  and  $V_{\text{th}}$  were calculated in the saturation regime (drain voltage,  $V_D$  = -40 V) using the equation  $I_D = \mu_{\text{FET}} C_i W (2L)^{-1} (V_G - V_{\text{th}})^2$ , where  $C_i$  is the capacitance of the dielectric sandwiched between the Au dots and highly doped *n*-type (100) Si substrate, was measured using an Agilent 4284 precision LCR meter.

## 3. RESULTS AND DISCUSSION

Most inorganic oxides (e.g., SiO<sub>2</sub>, Al<sub>2</sub>O<sub>3</sub>) or high- $\kappa$  polymer dielectrics having hydrophilic surface characteristics, i.e., high surface energy ( $\gamma$ ), inhibit the preferential edge-on crystal growth of  $\pi$ -conjugated polymers. It has been reported that slight differences in molecular interactions at the semiconductor-dielectric interface drastically changed the crystalline structures of both vacuum- and solution-processed organic semiconductors in terms of crystallinity, GBs, and crystal orientation.<sup>11,12,15–17</sup> To minimize the interfacial mismatches, high- $\gamma$  surfaces have usually been treated with SAMs or polymers.<sup>11,12,15–17</sup> For solution-processable organic semiconductors, it is necessary for the polymer-modified surfaces to maintain a consistent wettability against the hydrophilic oxides. This is achieved by grafting polymers to active moieties on the surfaces or cross-linking the polymer.<sup>11,12,18–20,27–29</sup>

As mentioned earlier, MPTS has a trimethoxysilane (TS) moiety, which is one of the most important grafting sites for coupling polymers to oxide surfaces. In the present study, MPTS was copolymerized with St to create PSMPTS copolymers. Table 1 shows characteristics of the synthesized PSMPTS copolymers.  $M_n$  of the PSMPTS copolymers ranged from 13 400 to 34 000 g mol<sup>-1</sup>, as determined by GPC analysis (see Figure S1 in the Supporting Information). The mol % of each monomer in the PSMPTS copolymers was determined by <sup>1</sup>H NMR spectra showing different integration ratios of

**Table 1.** Typical Characteristics of a PSMPTS Copolymer Series Synthesized in This Study

notation	feed ratio [St] <sub>0</sub> /[MPTS] <sub>0</sub>	mol %		M <sub>n</sub> (g mol <sup>-1</sup> )	M <sub>w</sub> / M <sub>n</sub>	T <sub>g</sub> (°C)
		St	MPTS			
PSMPTS-5	99/1	95	5	13400	2.03	86.1
PSMPTS-8	98/2	92	8	15900	2.18	84.8
PSMPTS-11 <sup>a</sup>	97/3	89	11	32700	2.71	78.3

<sup>a</sup>AIBN (1 wt %), 60 °C, 24 h.

aromatic proton peaks at 6.5 and 7.1 ppm (for the St units) and a methyl peak at 3.6 ppm (for the MPTS units) (see Figure S2 in the Supporting Information). The molar compositions of MPTS units in the copolymers were 5, 8, and 11%, respectively. Based on the GPC and <sup>1</sup>H NMR results, it was estimated that all of the copolymers contained at least 6 (for PSMPTS-5) and up to 30 (for PSMPTS-11) TS moieties per chain. This would presumably allow much more rapid grafting of the copolymers to a SiO<sub>2</sub> surface than silane-coupled polymers with a single chlorosilane moiety. As the MPTS mol % increased, the glass transition temperature (T<sub>g</sub>) of PSMPTS as determined by DSC monotonically decreased (see Figure S3 in the Supporting Information).

To investigate the grafting efficiency of the copolymers to hydroxyl-group on the surface, PSMPTS solutions were spin-cast onto a UVO<sub>3</sub>-treated 300 nm-thick SiO<sub>2</sub> layer on a heavily *n*-doped Si substrate. The resulting 20–30 nm thick PSMPTS films were then annealed at 150 °C for *t*<sub>ANN</sub> = 60 min. The annealed films were subsequently rinsed with an excess of toluene to remove any uncoupled PSMPTS residue from the SiO<sub>2</sub> surfaces (see the Experimental Section for more details).

Figure 2 shows AFM topographies of the untreated and PSMPTS-treated SiO<sub>2</sub> substrates. With the benefit of multiple

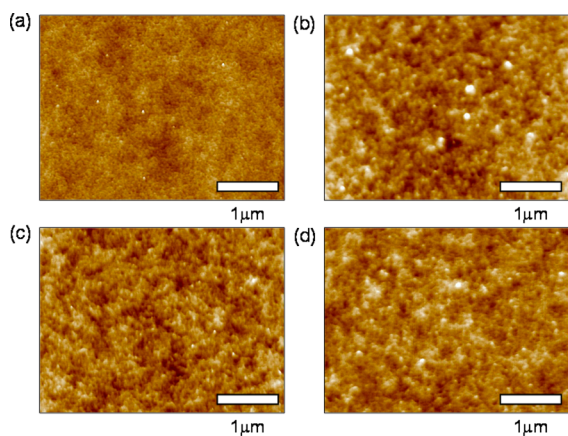


**Figure 2.** AFM topographies of (a) bare SiO<sub>2</sub> (*R*<sub>q</sub> = 0.27 nm) and (b–d) PSMPTS-treated SiO<sub>2</sub> bilayer dielectrics with different PSMPTS copolymer layers: (b) PSMPTS-5 (*R*<sub>q</sub> = 0.36 nm), (c) PSMPTS-8 (*R*<sub>q</sub> = 0.33 nm), and (d) PSMPTS-11 (*R*<sub>q</sub> = 0.30 nm).

TS coupling sites distributed throughout the PSMPTS chains, the copolymers were grafted to the SiO<sub>2</sub> surfaces in ambient air and formed relatively smooth polymer-coated layers with root-mean-square surface roughness (*R*<sub>q</sub>) values of 0.30–0.36 nm. However, the AFM topography of the end-grafted PS-Si(CH<sub>3</sub>)<sub>2</sub>Cl layer on the SiO<sub>2</sub> surface showed locally uncovered regions due to the air-sensitive chlorosilane moiety, resulting in

a relatively high *R*<sub>q</sub> value of 0.37 nm (see Figure S4a in the Supporting Information). As the MPTS composition in PSMPTS increased from 5 to 11 mol %, it was found that the *R*<sub>q</sub> values of the copolymer coated-SiO<sub>2</sub> surfaces decreased from 0.36 to 0.30 nm. PSMPTS-5, which had six coupling sites, yielded a low-grafting efficiency, showing irregularly polymer-coated regions (see Figure 2b). In contrast, PSMPTS-11, which had the highest number of coupling sites, seemed to be uniformly grafted to the SiO<sub>2</sub> surface and had a similar roughness level (*R*<sub>q</sub> = 0.30 nm) to that (0.27 nm) of the untreated SiO<sub>2</sub> surface.

Surface-grafted polymer layers, acting as organic interlayers between semiconducting films and inorganic oxide (or high-κ polymer) dielectrics, chemically deactivate or physically bury the number of polar moieties on the dielectric surfaces. It is known that end-functionalized polymers with a single coupling site form either brush or pancake type molecular layers on surfaces, and their thickness depends on the areal grafting density and chain length.<sup>30,31</sup> For the PSMPTS copolymers with multiple coupling sites, it was found that the thermal grafting time (*t*<sub>ANN</sub>) at 150 °C drastically changed the thicknesses of the grafted PSMPTS layers. Figure 3a shows

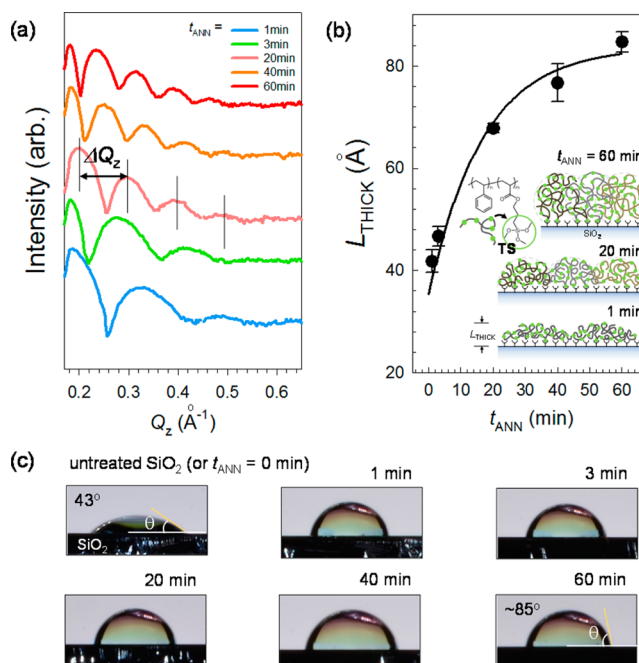


**Figure 3.** (a) X-ray reflectivity profiles of the PSMPTS-11 layers on SiO<sub>2</sub> surfaces and (b) the calculated values of *L*<sub>THICK</sub>. The inset represents the schemes of the conformation of grafted chains on the SiO<sub>2</sub> surfaces with an increase in *t*<sub>ANN</sub>. (c) Variation in water contact angle on the PSMPTS-11-treated SiO<sub>2</sub> bilayer as a function of *t*<sub>ANN</sub>.

XRR profiles of PSMPTS-11-treated SiO<sub>2</sub> bilayer dielectrics fabricated with *t*<sub>ANN</sub> ranging from 0 to 60 min in ambient air. All the XRR profiles for the grafted PSMPTS-11 layers showed discernible peak intervals,  $\Delta Q_z$ , ranging from 0.075 to 0.153 Å<sup>-1</sup>, which were used to calculate the layer thickness ( $L_{\text{THICK}} = 2\pi/\Delta Q_z$ ). *L*<sub>THICK</sub> tended to increase with increasing *t*<sub>ANN</sub>, with a maximum thicknesses of 84 Å observed for *t*<sub>ANN</sub> = 60 min, as shown in Figure 3b. After short-term annealing at 150 °C, e.g., 1 or 3 min, PSMPTS-11 was grafted to the SiO<sub>2</sub> surface layers with a thickness of more than 40 Å. Based on the *L*<sub>THICK</sub> variations of PSMPTS-11, which has a radius of gyration of

Table 2. Electrical Characteristics of P3HT OFETs Fabricated with Different Dielectrics

dielectric	surface modifier	dielectric roughness ( $R_q$ , nm)	$\mu_{\text{FET}}$ ( $\text{cm}^2 \text{V}^{-1} \text{s}^{-1}$ )	$V_{\text{th}}$ (V)	$I_{\text{on}}/I_{\text{off}}$
untreated $\text{SiO}_2$		0.27	$0.010 \pm 0.003$	13	$>10^5$
PS- $\text{Si}(\text{CH}_3)_2\text{Cl}$	26 kDa PS- $\text{Si}(\text{CH}_3)_2\text{Cl}$	0.37	$0.011 \pm 0.002$	10	$>10^5$
PSMPTS-treated $\text{SiO}_2$	PSMPTS-5	0.36	$0.011 \pm 0.003$	6	$>10^5$
	PSMPTS-8	0.33	$0.011 \pm 0.002$	4	$>10^5$
	PSMPTS-11	0.30	$0.012 \pm 0.002$	0	$>10^5$

approximately 10 nm, it was found that the grafting densities of PSMPTS-11 chains increased monotonically with an increase in  $t_{\text{ANN}}$  due to the randomly distributed TS coupling sites in the copolymer, as shown in the inset in Figure 3b. Figure 3c shows digital images of water droplets on these copolymer-grafted  $\text{SiO}_2$  surfaces. The untreated  $\text{SiO}_2$  and the polymer-treated surface that was not thermally annealed ( $t_{\text{ANN}} = 0$  min) still maintained a hydrophilic character, as determined by the low water contact angles ( $\theta_{\text{water}}$ ) of approximately  $43^\circ$ . In contrast, all the thermally grafted polymer- $\text{SiO}_2$  surfaces showed similar surface hydrophobicity, with  $\theta_{\text{water}}$  values of  $83\text{--}86^\circ$ . Based on these results, it is apparent that PSMPTS copolymers containing multiple coupling sites can undergo rapid multisite grafting to  $\text{SiO}_2$  surfaces, resulting in an increase in  $L_{\text{THICK}}$  as a function of  $t_{\text{ANN}}$ .

To develop a uniformly grafted layer of the PSMPTS copolymers to hydroxyl groups on the  $\text{SiO}_2$  dielectric, spun-cast PSMPTS films were treated at  $150^\circ\text{C}$  for 60 min and subsequently rinsed with an excess of toluene. All the PSMPTS- $\text{SiO}_2$  bilayer dielectrics had  $C_i$  values between  $10.4$  and  $10.8 \text{ nF cm}^{-2}$ , similar to that ( $10.9 \text{ nF cm}^{-2}$ ) of the untreated 300 nm-thick  $\text{SiO}_2$  layer due to ultrathin polymeric layer, i.e.,  $50\text{--}84 \text{ \AA}$  (see Table 2).

As semiconducting channel layers, solution-processed P3HT films can contain various complex microstructures depending on the solvent solubility, solvent evaporation rate, and processing temperature. Recently, it has been reported that a fast crystallization of strongly  $\pi$ -conjugated P3HT can be induced by ultrasonication in a dilute P3HT solution.<sup>32–34</sup> To fabricate well-interconnected nanofibril crystallites of  $\pi$ -conjugated P3HT ( $M_n = 21\,000 \text{ g mol}^{-1}$ ,  $M_w/M_n = 1.17$ ) on the gate dielectrics, a solution of 0.2 wt % P3HT in toluene was first ultrasonicated in a double jacketed beaker maintained at  $18^\circ\text{C}$  for 10 min. This ultrasonicated solution was then spun-cast onto all the  $\text{SiO}_2$  gate dielectrics. Figure 4 shows AFM topographies of the ultrasound-assisted P3HT crystallites spun-cast on the untreated and PSMPTS-treated  $\text{SiO}_2$  dielectrics. On the untreated and PSMPTS-treated  $\text{SiO}_2$  surfaces showing different surface roughnesses and energies, P3HT nanofibrils were highly extended and percolated, with a lateral width of  $24\text{--}30 \text{ nm}$ . The similar crystal morphologies of P3HT on these gate dielectrics were mainly related to the directed self-assembly of P3HT in the previously ultrasonicated solution.<sup>32,33</sup>

Synchrotron-based GIXD analysis was also performed to evaluate the  $\pi$ -conjugated orientations of P3HT in these films (see Figure 5). 2D GIXD patterns of the ultrasound-assisted P3HT films spun-cast on the dielectrics showed intense out-of-plane and in-plane X-ray reflections along the  $Q_z$  and  $Q_{xy}$  axes, respectively. It should be noted that the beam center and (100) peak position of the patterns were blocked with an Al beam stopper to avoid any detector saturation due to the strong X-ray reflections. The ( $h00$ ) and (010) reflections along the  $Q_z$  and  $Q_{xy}$  axes, respectively, corresponded to a multistacked crystal

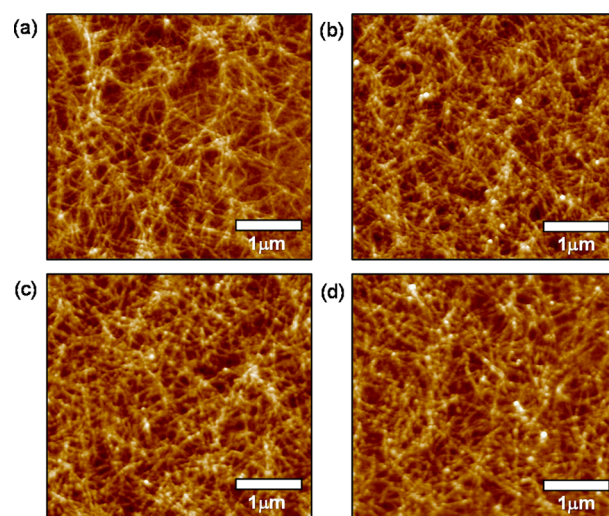


Figure 4. AFM topographies of ultrasound-assisted P3HT films spun-cast on (a) untreated and (b–d) PSMPTS-treated  $\text{SiO}_2$  bilayer dielectrics: (b) PSMPTS-5, (c) PSMPTS-8, and (d) PSMPTS-11.

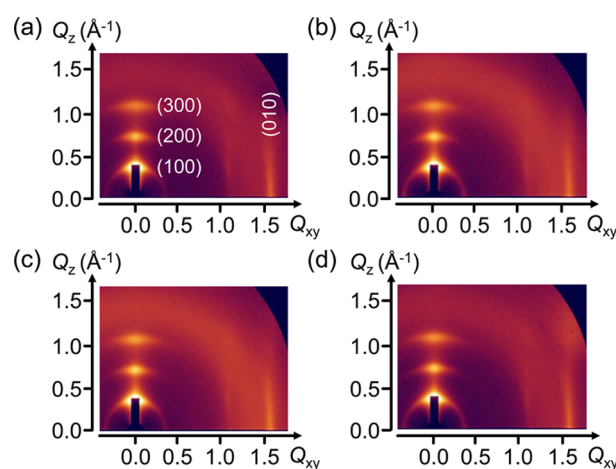
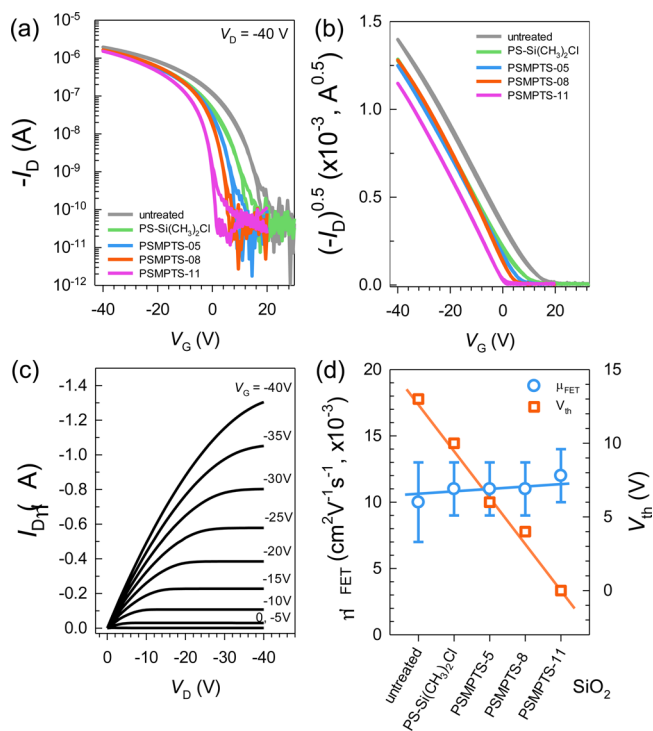


Figure 5. 2D GIXD patterns of the ultrasound-assisted P3HT films spun-cast on different gate dielectrics: (a) untreated  $\text{SiO}_2$ , (b) PSMPTS-5  $\text{SiO}_2$ , (c) PSMPTS-8  $\text{SiO}_2$ , and (d) PSMPTS-11  $\text{SiO}_2$ .

structure, where “edge-on” P3HT chains were preferentially oriented with a (100) layer spacing of about  $16.6 \text{ \AA}$  and an intermolecular  $\pi\text{--}\pi$  distance of  $\sim 3.80 \text{ \AA}$ .<sup>35</sup> As expected from the AFM morphologies in Figure 4, all the 2D GIXD patterns of the ultrasound-assisted P3HT films were similar to each other in intensity and orientation. The similarities between P3HT crystallites formed in the ultrasound-assisted films, including crystallinity,  $\pi$ -conjugated orientation, and crystal interconnection, may provide density of states in the conducting channel similar to those previously observed,<sup>36,37</sup> suggesting that these P3HT films on the different gate dielectrics might have similar structural charge traps.

Top-contacted electrode OFETs were fabricated by the thermal evaporation of Au through a shadow mask ( $L = 100 \mu\text{m}$ ;  $W = 1500 \mu\text{m}$ ) onto the P3HT films. Figure 6 shows the



**Figure 6.** (a–c) Electrical performances of P3HT OFETs: (a)  $I_D$ – $V_G$  transfer curves and (b) the resulting  $I_D^{0.5}$ – $V_G$  plots, (c)  $I_D$ – $V_D$  output curves of the PSMPTS-11-treated  $\text{SiO}_2$  system, and (d) variations of  $\mu_{\text{FET}}$  and  $V_{\text{th}}$  of the P3HT OFETs fabricated on untreated, PS-Si( $\text{CH}_3$ ) $_2$ Cl-, and PSMPTS-treated  $\text{SiO}_2$  dielectrics.

electrical characteristics of the P3HT OFETs for all the gate dielectrics. First, the drain current–gate voltage ( $I_D$ – $V_G$ ) transfer curves of the P3HT OFETs based on untreated, 26 kDa PS-Si( $\text{CH}_3$ ) $_2$ Cl- and PSMPTS-treated  $\text{SiO}_2$  dielectrics were measured in the saturation regime (drain voltage,  $V_D = -40 \text{ V}$ ) (see Figure 6a). Based on the resulting  $I_D^{0.5}$ – $V_G$  plots (see Figure 6b), the electrical properties of the OFETs, including  $\mu_{\text{FET}}$ ,  $V_{\text{th}}$ , and  $I_{\text{ON}}/I_{\text{OFF}}$ , were determined and are summarized in Table 2. OFETs with typical *p*-type transistor characteristics (see Figure 6c) yielded similar  $\mu_{\text{FET}}$  values of  $0.010$ – $0.012 \text{ cm}^2 \text{ V}^{-1} \text{ s}^{-1}$ , as well as negligible  $V_G$ -sweep hysteresis. However,  $V_{\text{th}}$  values were drastically shifted to the negative direction from  $+13 \text{ V}$  (for untreated  $\text{SiO}_2$ ) and  $+10 \text{ V}$  (for 26 kDa PS-Si( $\text{CH}_3$ ) $_2$ Cl-treated  $\text{SiO}_2$ ) to  $0 \text{ V}$  (for the PSMPTS-11-treated  $\text{SiO}_2$ ). The PSMPTS-11-treated  $\text{SiO}_2$  system with an  $84 \text{ \AA}$ -thick PS-based interlayer showed the best electrical performance ( $\mu_{\text{FET}} = 0.012 \text{ cm}^2 \text{ V}^{-1} \text{ s}^{-1}$ ,  $V_{\text{th}} = 0 \text{ V}$ , and  $I_{\text{on}}/I_{\text{off}} > 10^5$ ).

Because the crystalline morphologies and  $\pi$ -conjugated orientations of the P3HT layers were very similar among all the dielectrics, the  $V_{\text{th}}$  shift of the P3HT OFETs was mainly related to the variations in trap density at the semiconductor–dielectric interface. The interfacial traps are usually due to surface imperfections of the dielectrics, such as polar moieties. As interfacial trap sites, hydroxyl groups on an untreated  $\text{SiO}_2$  layer could be passivated by the PSMPTS copolymer chains chemically coupled with the hydroxyl groups. As the coupling densities of the PSMPTS chains increased on the  $\text{SiO}_2$  surfaces,

the decrease of the hydroxyl groups at the P3HT–dielectric interface induced a negative shift in  $V_{\text{th}}$ .<sup>38</sup> Similarly, the 26 kDa PS-Si( $\text{CH}_3$ ) $_2$ Cl chains under an inert condition ( $\text{H}_2\text{O} < 0.1 \text{ ppm}$ ;  $\text{O}_2 < 0.1 \text{ ppm}$ ) could efficiently passivate the polar moieties on the  $\text{SiO}_2$  surface due to the improved coupling activity of the air-sensitive chlorosilane site. The corresponding P3HT OFET showed the  $V_{\text{th}}$  value of  $-1 \text{ V}$ , in comparison to  $+10 \text{ V}$  of the air-processed PS-Si( $\text{CH}_3$ ) $_2$ Cl-treated system (see Figure S5 in the Supporting Information).

In summary, the introduction of ultrathin polymer interlayers between solution-processed semiconductors and a polar dielectric surface was successfully demonstrated to optimize the electrical properties of solution-processed polymer FETs. Ambient-air grafting of solution-processable PS-based random copolymers with multiple coupling sites allowed for physicochemically stable polymer layers on hydroxyl group containing  $\text{SiO}_2$  surfaces. The optimization of thermally grafted PSMPTS layers drastically reduced the interfacial charge traps in OFETs.

#### 4. CONCLUSIONS

As dielectric modifiers, various PSMPTS copolymers with MPTS units of 5–11 mol % were synthesized by a free radical polymerization of styrene and MPTS. The PSMPTS copolymers were spun-cast onto hydroxyl-groups presenting  $\text{SiO}_2$  dielectrics, annealed at  $150 \text{ }^\circ\text{C}$ , and subsequently rinsed with an excess of toluene. Interestingly, PSMPTS-11 was thermally grafted when exposed to high temperature for more than 1 min and formed a much denser hydrophobic layer on the  $\text{SiO}_2$  surface with an increase in annealing time. A preultrasonicated P3HT solution was spun-cast on all the dielectrics, and the ultrasound-assisted P3HT films showed a highly interconnected networks of P3HT nanofibrils, where most of the semi-conducting polymer chains were preferentially oriented with an “edge-on” conformation. The resulting P3HT OFETs showed similar  $\mu_{\text{FET}}$  values of  $0.01$ – $0.012 \text{ cm}^2 \text{ V}^{-1} \text{ s}^{-1}$ . However, values of  $V_{\text{th}}$ , related to the interface polar charge traps, were drastically changed from  $+13 \text{ V}$  (for untreated  $\text{SiO}_2$ ) to  $0 \text{ V}$  (for the PSMPTS-treated  $\text{SiO}_2$ ). These results strongly suggest that the facile and rapid grafting of PS-based copolymers onto  $\text{SiO}_2$  dielectrics in ambient air can be used as a continuous solution-based dielectric treatment for large-scale OFET fabrication.

#### ■ ASSOCIATED CONTENT

##### Supporting Information

GPC,  $^1\text{H}$  NMR and DSC analyses, AFM topographies, and typical  $I_D$ – $V_G$  transfer curves of P3HT OFET. This material is available free of charge via the Internet at <http://pubs.acs.org>.

#### ■ AUTHOR INFORMATION

##### Corresponding Authors

\*(H.Y.) E-mail: [hcyang@inha.ac.kr](mailto:hcyang@inha.ac.kr). Phone: +82-32-860-7494  
\*(J.H.Y.) E-mail: [youk@inha.ac.kr](mailto:youk@inha.ac.kr). Phone: +82-32-860-7498.

##### Notes

The authors declare no competing financial interest.

#### ■ ACKNOWLEDGMENTS

This work was supported by grants from the Center for Advanced Soft Electronics under the Global Frontier Research Program (2012M3A6A5055225), Basic Science Research Program through the National Research Foundation of Korea

(NRF) funded by MEST (NRF-2013R1A1A2006392, NRF-2013RA1A12063963).

## ■ ABBREVIATIONS

AFM, atomic force microscopy  
GB, grain boundary  
GIXD, grazing-incidence X-ray diffraction  
 $M_n$ , Number-average molecular weight  
OFET, organic field-effect transistor  
P3HT, poly(3-hexyl thiophene)  
PS, polystyrene  
PSMPTS, polystyrene-random-poly(3-methacryloxypropyl-trimethoxysilane)  
SiO<sub>2</sub>, silicon dioxide  
TS, trimethoxysilane

## ■ REFERENCES

- (1) Gelinck, G. H.; Huitema, H. E. A.; van Veenendaal, E.; Cantatore, E.; Schrijnemakers, L.; van der Putten, J. B. P. H.; Geuns, T. C. T.; Beenhakkers, M.; Giesbers, J. B.; Huisman, B.-H.; Meijer, E. J.; Benito, E. M.; Touwslager, F. J.; Marsman, A. W.; van Rens, B. J. E.; de Leeuw, D. M. Flexible Active-Matrix Displays and Shift Registers Based on Solution-Processed Organic Transistors. *Nat. Mater.* **2004**, *3*, 106–110.
- (2) Huitema, H. E. A.; Gelinck, G. H.; van der Putten, J. B. P. H.; Kuijk, K. E.; Hart, C. M.; Cantatore, E.; Herwig, P. T.; van Breemen, A. J. J. M.; de Leeuw, D. M. Plastic Transistors in Active-Matrix Displays - The Handling of Grey Levels by These Large Displays Paves the Way for Electronic Paper. *Nature* **2001**, *414*, 599–599.
- (3) Rogers, J. A.; Bao, Z.; Baldwin, K.; Dodabalapur, A.; Crone, B.; Raju, V. R.; Kuck, V.; Katz, H.; Amundson, K.; Ewing, J.; Drzaic, P. Paper-like Electronic Displays: Large-Area Rubber-Stamped Plastic Sheets of Electronics and Microencapsulated Electrophoretic Inks. *Proc. Natl. Acad. Sci. U. S. A.* **2001**, *98*, 4835–4840.
- (4) Comiskey, B.; Albert, J. D.; Yoshizawa, H.; Jacobson, J. An Electrophoretic Ink for All-Printed Reflective Electronic Displays. *Nature* **1998**, *394*, 253–255.
- (5) Sokolov, A. N.; Roberts, M. E.; Bao, Z. Fabrication of Low-Cost Electronic Biosensors. *Mater. Today* **2009**, *12*, 12–20.
- (6) Facchetti, A. Pi-Conjugated Polymers for Organic Electronics and Photovoltaic Cell Applications. *Chem. Mater.* **2011**, *23*, 733–758.
- (7) Knopfmacher, O.; Hammock, M. L.; Appleton, A. L.; Schwartz, G.; Mei, J. G.; Lei, T.; Pei, J.; Bao, Z. Highly Stable Organic Polymer Field-Effect Transistor Sensor for Selective Detection in the Marine Environment. *Nat. Commun.* **2014**, *5*, 2954.
- (8) Wang, C. L.; Dong, H. L.; Hu, W. P.; Liu, Y. Q.; Zhu, D. B. Semiconducting Pi-Conjugated Systems in Field-Effect Transistors: A Material Odyssey of Organic Electronics. *Chem. Rev.* **2012**, *112*, 2208–2267.
- (9) Sirringhaus, H. 25th Anniversary Article: Organic Field-Effect Transistors: The Path Beyond Amorphous Silicon. *Adv. Mater.* **2014**, *26*, 1319–1335.
- (10) Kang, I.; Yun, H. J.; Chung, D. S.; Kwon, S. K.; Kim, Y. H. Record High Hole Mobility in Polymer Semiconductors via Side-Chain Engineering. *J. Am. Chem. Soc.* **2013**, *135*, 14896–14899.
- (11) Kim, S. H.; Jang, M.; Yang, H.; Anthony, J. E.; Park, C. E. Physicochemically Stable Polymer-Coupled Oxide Dielectrics for Multipurpose Organic Electronic Applications. *Adv. Funct. Mater.* **2011**, *21*, 2198–2207.
- (12) Jang, M.; Park, J. H.; Im, S.; Kim, S. H.; Yang, H. Critical Factors to Achieve Low Voltage- and Capacitance-based Organic Field-Effect Transistors. *Adv. Mater.* **2014**, *26*, 288–292.
- (13) Li, J.; Zhao, Y.; Tan, H. S.; Guo, Y.; Di, C.-A.; Yu, G.; Liu, Y.; Lin, M.; Lim, S. H.; Zhou, Y.; Su, H.; Ong, B. S. A Stable Solution-Processed Polymer Semiconductor with Record High-Mobility for Printed Transistors. *Sci. Rep.* **2012**, *2*, 754.
- (14) Kim, S. H.; Jang, M.; Yang, H.; Park, C. E. Effect of Pentacene-Dielectric Affinity on Pentacene Thin Film Growth Morphology in Organic Field-Effect Transistors. *J. Mater. Chem.* **2010**, *20*, 5612–5620.
- (15) Yang, H.; Kim, S. H.; Yang, L.; Yang, S. Y.; Park, C. E. Pentacene Nanostructures on Surface-Hydrophobicity-Controlled Polymer/SiO<sub>2</sub> Bilayer Gate-Dielectrics. *Adv. Mater.* **2007**, *19*, 2868–2872.
- (16) Yoon, M. H.; Kim, C.; Facchetti, A.; Marks, T. J. Gate Dielectric Chemical Structure-Organic Field-Effect Transistor Performance Correlations for Electron, Hole, and Ambipolar Organic Semiconductors. *J. Am. Chem. Soc.* **2006**, *128*, 12851–12869.
- (17) Yang, H.; Shin, T. J.; Ling, M. M.; Cho, K.; Ryu, C. Y.; Bao, Z. Conducting AFM and 2D GIXD Studies on Pentacene Thin Films. *J. Am. Chem. Soc.* **2005**, *127*, 11542–11543.
- (18) Chung, S.; Jang, M.; Ji, S. B.; Im, H.; Seong, N.; Ha, J.; Kwon, S. K.; Kim, Y. H.; Yang, H.; Hong, Y. Flexible High-Performance All-Inkjet-Printed Inverters: Organo-Compatible and Stable Interface Engineering. *Adv. Mater.* **2013**, *25*, 4773–4777.
- (19) Park, S. H.; Lee, H. S.; Kim, J. D.; Breiby, D. W.; Kim, E.; Park, Y. D.; Ryu, D. Y.; Lee, D. R.; Cho, J. H. A Polymer Brush Organic Interlayer Improves the Overlying Pentacene Nanostructure and Organic Field-Effect Transistor Performance. *J. Mater. Chem.* **2011**, *21*, 15580–15586.
- (20) Li, L. Q.; Hu, W. P.; Chi, L. F.; Fuchs, H. Polymer Brush and Inorganic Oxide Hybrid Nanodielectrics for High Performance Organic Transistors. *J. Phys. Chem. B* **2010**, *114*, 5315–5319.
- (21) Jennings, A. R.; Bassampour, Z. S.; Patel, A. G.; Son, D. Y. Orthogonal Reactivity of Thiols toward Chlorovinylsilanes: Selective Thiol-End Chemistry. *Tetrahedron Lett.* **2014**, *55*, 6773–6775.
- (22) Zhang, F.; Hou, G. H.; Dai, S. J.; Lu, R.; Wang, C. C. Preparation of Thermosensitive PNIPAM Microcontainers and a Versatile Method to Fabricate PNIPAM Shell on Particles with Silica Surface. *Colloid Polym. Sci.* **2012**, *290*, 1341–1346.
- (23) Alam, M. A.; Takafuji, M.; Ihara, H. Thermosensitive Hybrid Hydrogels with Silica Nanoparticle-Cross-Linked Polymer Networks. *J. Colloid Interface Sci.* **2013**, *405*, 109–117.
- (24) Zhang, J. T.; Pan, C. J.; Keller, T.; Bhat, R.; Gottschaldt, M.; Schubert, U. S.; Jandt, K. D. Monodisperse, Temperature-Sensitive Microgels Crosslinked by Si-O-Si Bonds. *Macromol. Mater. Eng.* **2009**, *294*, 396–404.
- (25) Xuan, F. Q.; Liu, J. S.; Xu, T. W. Preparation and Characterization of Novel Negatively Charged Hybrid Membranes. *Polym. Adv. Technol.* **2011**, *22*, 554–559.
- (26) Jeffries-El, M.; Sauve, G.; McCullough, R. D. In-Situ End-Group Functionalization of Regioregular Poly(3-alkylthiophene) Using the Grignard Metathesis Polymerization Method. *Adv. Mater.* **2004**, *16*, 1017–1019.
- (27) Kim, S. H.; Hong, K.; Jang, M.; Jang, J.; Anthony, J. E.; Yang, H.; Park, C. E. Photo-Curable Polymer Blend Dielectrics for Advancing Organic Field-Effect Transistor Applications. *Adv. Mater.* **2010**, *22*, 4809–4813.
- (28) Kim, S. H.; Jang, M.; Kim, J.; Choi, H.; Baek, K. Y.; Park, C. E.; Yang, H. Complementary Photo and Temperature Cured Polymer Dielectrics with High-Quality Dielectric Properties for Organic Semiconductors. *J. Mater. Chem.* **2012**, *22*, 19940–19947.
- (29) Lee, T.-W.; Shin, J. H.; Kang, I.-N.; Lee, S. Y. Photocurable Organic Gate Insulator for the Fabrication of High-Field Effect Mobility Organic Transistors by Low Temperature and Solution Processing. *Adv. Mater.* **2007**, *19*, 2702–2706.
- (30) Minko, S. Responsive Polymer Brushes. *Polym. Rev.* **2006**, *46*, 397–420.
- (31) Pinto, J. C.; Whiting, G. L.; Khodabakhsh, S.; Torre, L.; Rodriguez, A.; Dalglish, R. M.; Higgins, A. M.; Andreasen, J. W.; Nielsen, M. M.; Geoghegan, M.; Huck, W. T. S.; Sirringhaus, H. Organic Thin Film Transistors with Polymer Brush Gate Dielectrics Synthesized by Atom Transfer Radical Polymerization. *Adv. Funct. Mater.* **2008**, *18*, 36–43.

(32) Aiyar, A. R.; Hong, J. I.; Nambiar, R.; Collard, D. M.; Reichmanis, E. Tunable Crystallinity in Regioregular Poly(3-hexylthiophene) Thin Films and Its Impact on Field Effect Mobility. *Adv. Funct. Mater.* **2011**, *21*, 2652–2659.

(33) Aiyar, A. R.; Hong, J. I.; Izumi, J.; Choi, D.; Kleinhenz, N.; Reichmanis, E. Ultrasound-Induced Ordering in Poly(3-hexylthiophene): Role of Molecular and Process Parameters on Morphology and Charge Transport. *ACS Appl. Mater. Interfaces* **2013**, *5*, 2368–2377.

(34) Kim, B. G.; Kim, M. S.; Kim, J. Ultrasonic-Assisted Nanodimensional Self-Assembly of Poly-3-hexylthiophene for Organic Photovoltaic Cells. *ACS Nano* **2010**, *4*, 2160–2166.

(35) Yang, H. C.; Shin, T. J.; Yang, L.; Cho, K.; Ryu, C. Y.; Bao, Z. N. Effect of Mesoscale Crystalline Structure on the Field-Effect Mobility of Regioregular Poly(3-hexyl thiophene) in Thin-Film Transistors. *Adv. Funct. Mater.* **2005**, *15*, 671–676.

(36) McGehee, M. D.; Heeger, A. J. Semiconducting (Conjugated) Polymers as Materials for Solid-State Lasers. *Adv. Mater.* **2000**, *12*, 1655–1668.

(37) Rivnay, J.; Noriega, R.; Northrup, J. E.; Kline, R. J.; Toney, M. F.; Salleo, A. Structural Origin of Gap States in Semicrystalline Polymers and the Implications for Charge Transport. *Phys. Rev. B* **2011**, *83*, 121306.

(38) Yoon, M.-H.; Kim, C.; Facchetti, A.; Marks, T. J. Gate Dielectric Chemical Structure-Organic Field-Effect Transistor Performance Correlation for Electron, Hole, and Ambipolar Organic Semiconductor. *J. Am. Chem. Soc.* **2006**, *128*, 12851–12869.